THE JOURNAL OF BIOLOGICAL CHEMISTRY
Vol. 279, No. 9, Issue of February 27, pp. 7917–7924, 2004
Printed in U.S.A.

Association of the Chaperone αB-crystallin with Titin in Heart Muscle*

Received for publication, July 11, 2003, and in revised form, November 10, 2003
Published, JBC Papers in Press, December 4, 2003, DOI 10.1074/jbc.M307473200

Belinda Bullard‡§, Charles Ferguson‡, Ave Minajeva¶, Mark C. Leake¶‖, Mathias Gautel‡, Dietmar Labeit‡‡, Linlin Ding§§, Siegfried Labeit‡‡, Joseph Horwitz§§, Kevin R. Leonard‡, and Wolfgang A. Linke¶‖‖**

From the ‡European Molecular Biology Laboratory, Meyerhofstrasse 1, D-69117 Heidelberg, Germany, the ¶Institute of Physiology and Pathophysiology, University of Heidelberg, D-69120 Heidelberg, Germany, the ‡‡Institut für Anasthesiologie und Operative Intensivmedizin, Universitätsklinikum, D-68135 Mannheim, Germany, and the §§Jules Stein Eye Institute, UCLA, Los Angeles, California 90024

αB-crystallin, a major component of the vertebrate lens, is a chaperone belonging to the family of small heat shock proteins. These proteins form oligomers that bind to partially unfolded substrates and prevent denaturation. αB-crystallin in cardiac muscle binds to myofibrils under conditions of ischemia, and previous work has shown that the protein binds to titin in the I-band of cardiac fibers (Golenhofen, N., Arbeiter, A., Koob, R., and Drenckhahn, D. (2002) *J. Mol. Cell. Cardiol.* 34, 309–319). This part of titin extends as muscles are stretched and is made up of immunoglobulin-like modules and two extensible regions (N2B and PEVK) that have no well defined secondary structure. We have followed the position of αB-crystallin in stretched cardiac fibers relative to a known part of the titin sequence. αB-crystallin bound to a discrete region of the I-band that moved away from the Z-disc as sarcomeres were extended. In the physiological range of sarcomere lengths, αB-crystallin bound in the position of the N2B region of titin, but not to PEVK. In overstretched myofibrils, it was also in the Ig region between N2B and the Z-disc. Binding between αB-crystallin and N2B was confirmed using recombinant titin fragments. The Ig domains in an eight-domain fragment were stabilized by αB-crystallin; atomic force microscopy showed that higher stretching forces were needed to unfold the domains in the presence of the chaperone. Reversible association with αB-crystallin would protect I-band titin from stress liable to cause domain unfolding until conditions are favorable for refolding to the native state.

αB-crystallin is one of several crystallins in the vertebrate lens. An important function of the protein is to act as a chaperone preventing partially unfolded proteins from forming aggregates that would make the lens opaque (1, 2). αB-crystallin is a member of the family of small heat shock proteins (sHSPs)[1]. These are chaperones in multisubunit complexes that bind to proteins in the early stages of denaturation, holding them in a folding-competent state. αB-crystallin is also found in tissues other than the lens, including cardiac and skeletal muscle (3). The αB-crystallin content of cardiac muscle is 3–5% of the total soluble protein (4), and it protects the fibers from the effects of ischemia, preventing extensive structural damage (5–7). αB-crystallin moves from general distribution in the cytosol to myofibrils following ischemia (8, 9). Recent immunoelectron microscopy of rat heart has shown that αB-crystallin is in a narrow region of the I-band rather than in the Z-disc, as was previously thought, and is also associated with desmin filaments connecting neighboring myofibrils (10). When actin was extracted from pig heart myofibrils, αB-crystallin remained, suggesting that the protein was associated with titin in the I-band rather than with actin; and this was supported by co-purification of αB-crystallin with titin (10).

Titin is a large (3 MDa) protein in striated muscle that spans half the sarcomere, forming an extensible link between the Z-disc and the thick filaments (11, 12). The molecule is largely made up of repeating modules composed of Ig- and fibronectin-like domains. The passive tension in muscle fibers is due to the part of titin that is in the I-band. In cardiac titin, this part of the sequence is made up of tandem Ig domains; an extensible PEVK domain, which is mostly random coil; and the N2B region, in which a central unique sequence (uN2B) is flanked by Ig domains (see Fig. 1) (13, 14). When cardiac myofibrils are stretched, the different parts of I-band titin extend sequentially: tandem Ig regions straighten out; the PEVK domain is pulled out; and the N2B region extends last (15, 16). The elasticity of cardiac muscle is affected by the relative amount of two titin isoforms: the N2B isoform, which has two tandem Ig regions separated by the N2B region together with a short PEVK domain, and the N2BA isoform, which has additional tandem Ig regions and an N2A region on the N-terminal side of a longer PEVK domain (see Fig. 1) (17, 18). The predominant isoform in rabbit heart is N2B, which makes up >80% of the total titin.

The parts of cardiac titin most likely to associate with αB-crystallin are the PEVK domain and uN2B region. αB-crystallin binds to proteins that have non-native secondary structure, and these regions of titin have no well defined structure. Another possible target is the less stable Ig domains in the proximal Ig region. When rabbit cardiac myofibrils are stretched, Ig domains in the proximal region start to unfold at the upper

* This work was supported by grants from the Deutsche Forschungsgemeinschaft (to M. G., S. L., and W. A. L.) and from the National Institutes of Health (to J. H.). The costs of publication of this article were defrayed in part by the payment of page charges. This article must therefore be hereby marked "*advertisement*" in accordance with 18 U.S.C. Section 1734 solely to indicate this fact.

§ To whom correspondence should be addressed. Tel.: 49-6221-387-268; Fax: 49-6221-387-306; E-mail: bullard@embl.de.

‖ Present address: Clarendon Lab., University of Oxford, Parks Rd., Oxford OX1 3PU, UK.

** Present address: Randall Centre, New Hunt's House, King's College, Guy's Campus, London SE1 1UL, UK.

‖‖ Present address: Muscle Biology, University of Münster, Schlossplatz 5, D-48419, Münster, Germany.

[1] The abbreviations used are: sHSPs, small heat shock proteins; uN2B, unique N2B; GdnHCl, guanidine hydrochloride; AFM, atomic force microscopy; pN, piconewtons.

limit of physiological sarcomere length (19), which would leave them prone to denaturation. The aim of this study was to determine to which part of titin the chaperone binds *in vivo*. As PEVK and N2B are the most extensible regions, αB-crystallin bound to either would affect the passive tension of cardiac fibers with consequences for the function of the heart.

EXPERIMENTAL PROCEDURES

Preparation of Proteins, Titin Constructs, and Antibodies—Titin was isolated from rabbit hearts by the method described previously (20). Titin fragments used in binding assays were derived from the sequence of human cardiac titin (13, 14), with the same numbering of domains. The constructs used were the same as those described previously (21, 22) and were expressed in *Escherichia coli* BL21(DE) pLysS cells (Stratagene): I24/I25 (two Ig domains flanking a short unique sequence in the N2B region; formally called I16/I17), I26/I27 (two Ig domains C-terminal to the uN2B region; formally called I18/I19), I26/I27–I84 (the PEVK domain common to N2BA and N2B of cardiac titin flanked by two N-terminal Ig domains and one C-terminal Ig domain; formally called I18/I19-I20), I84 (one Ig domain; formally called I20), and skeletal PEVK (a PEVK fragment of skeletal muscle titin). The uN2B construct (the unique sequence in the central N2B region) was expressed and purified using a similar method (23). A block of tandem Ig domains, I91–I98 (formally I27–I34), was prepared as described (24).

Recombinant human αB-crystallin was expressed in *E. coli* and purified as described (25). The antibody to αB-crystallin used was a rabbit polyclonal antibody raised against recombinant αB-crystallin; IgG was isolated from the serum by affinity chromatography. The mouse monoclonal antibodies used for immunolocalization and immunoaffinity assays were as follows: S54/56 and anti-I26 (I18/23) (26) and anti-I25 (15). The positions of the epitopes used for immunolocalization are shown in Fig. 1.

Preparation of Cardiac Myofibrils and Immunofluorescence Microscopy—-Myofibrils were prepared from the left ventricle of rabbit heart and skinned as described previously (15, 27). Trabeculae tied to glass rods were skinned in cold rigor solution with 0.5% Triton X-100 and then homogenized in rigor solution. A single myofibril was picked up from a drop of suspension on a coverslip with two glass needle tips coated with water-curing silicone adhesive using a Zeiss Axiovert 135 inverted microscope. Myofibrils were equilibrated at room temperature in a relaxing solution of 200 mM ionic strength at pH 7.1 (15). Leupeptin was included in all solutions to minimize titin degradation (28). Single myofibrils were stretched in relaxing solution to a particular sarcomere length and incubated with αB-crystallin (0.1 mg/ml) in relaxing solution for ~30 min. After washing in relaxing solution, myofibrils were incubated with anti-αB-crystallin IgG (0.1 mg/ml) for ~20 min, followed by Cy3-conjugated anti-rabbit IgG (diluted 1:50; Rockland Inc.); both were in relaxing solution. In double-labeling experiments, stretched myofibrils were incubated with anti-I25 (hybridoma supernatant diluted 1:5) and then αB-crystallin, followed by anti-αB-crystallin; incubations were for 20–30 min. The secondary antibodies used were Cy3-conjugated anti-mouse IgG and fluorescein isothiocyanate-conjugated anti-rabbit IgG (Rockland Inc.), both diluted 1:50. Images were recorded in the epifluorescence mode of the microscope using a 3CCD color video camera (Sony) and Scion Image software (Scion Corp.). The automatic integration feature of the CCD camera was used to superimpose three to five images during each recording. Epitope spacing was measured as described (28).

Immunoelectron Microscopy—Trabeculae were dissected from the left ventricle of rabbit heart 30 min after the rabbit was killed to allow development of ischemia and tied to glass rods in relaxing solution (0.1 M NaCl, 20 mM sodium phosphate (pH 7.0), 5 mM $MgCl_2$, 2 mM EGTA, and 5 mM ATP) so that the muscles were stretched by different amounts. Muscles were fixed in relaxing solution with 4% paraformaldehyde for 2 h at room temperature and processed as described previously (29). Frozen specimens were cryosectioned, and sections were labeled with anti-αB-crystallin IgG (0.1 mg/ml) or S54/56 hybridoma supernatant (diluted 1:5), followed by protein A complexed with 10-nm gold. Images were taken with a Philips 400T electron microscope at 80 kV. The distance from the center of the Z-disc to individual gold particles was measured on electron micrograph negatives for at least four myofibrils at each sarcomere length from 1.9 to 2.7 μm.

Immunoaffinity Binding Assay—αB-crystallin binding to titin was measured by an immunoaffinity method using protein A. Hybridoma supernatant containing monoclonal antibody to I26 was passed through a column of 200 μl of protein A-Sepharose CL-4B (Amersham Biosciences) equilibrated in binding buffer (0.1 M NaCl, 10 mM Tris-Cl (pH 7.2), 1 mM phenylmethylsulfonyl fluoride, and 0.1% Triton X-100). The protein A-Sepharose beads were washed, and aliquots of 50 μl were added to titin alone (10 μg), to titin (10 μg) plus αB-crystallin (5 μg), or to αB-crystallin alone (5 μg) in a total volume of 100 μl of binding buffer and incubated at 42 or 0 °C for 1 h. The beads were centrifuged for 3 min at 14,000 × *g*; and after removing the supernatant, they were washed three times with 500 μl of binding buffer. Protein bound to the beads was eluted by adding 50 μl of SDS-PAGE sample buffer; after heating for 3 min at 95 °C, the beads were centrifuged at 14,000 × *g* for 3 min, and the supernatant was run on a gel. An immunoblot was incubated with anti-αB-crystallin.

Circular Dichroism—The near-UV CD spectrum of I91–I98 was measured at 25, 37, 45, 50, and 55 °C. Protein was in 0.1 M NaCl and 50 mM sodium phosphate (pH 7.0). Spectra were recorded with a Jasco J600 CD spectrophotometer coupled with a Hewlett-Packard signal analyzer; 32 scans were averaged to reduce noise. Temperature was controlled by a water-jacketed cell of 10-mm path length. To study the effect of denaturation by GdnHCl, the near-UV CD spectrum of I91–I98 was measured in 0.1 M NaCl and 50 mM sodium phosphate (pH 7.0) at 25 °C. The protein was denatured by incubation in the same buffer with 6 M GdnHCl for 1 h at 25 °C, and the CD spectrum was recorded. The protein was renatured by exchanging with buffer without GdnHCl using a Centricon-30 (Amicon, Inc.), and the CD spectrum was measured again.

Electrophoresis and Immunoblotting—Gels (12% polyacrylamide) were run in the Laemmli buffer system and stained with Coomassie Blue or blotted onto nitrocellulose. Blots of titin fragments were incubated with αB-crystallin (0.1 mg/ml) in milk blocking buffer for 1 h; and after washing, they were incubated with anti-αB-crystallin serum (diluted 1:1000 in milk blocking buffer) for 1 h, washed again, and incubated with peroxidase-tagged goat anti-rabbit secondary antibody (diluted 1:50,000; Sigma). Reaction of recombinant proteins with αB-crystallin was determined from dot blots of native proteins. Recombinant proteins were spotted onto nitrocellulose; and after blocking in milk blocking buffer, the nitrocellulose was incubated with αB-crystallin, anti-αB-crystallin, and secondary antibody as described for blots of gels. Blots were developed with a luminescent substrate (ECL, Amersham Biosciences).

Atomic Force Microscopy (AFM)—Single molecule force spectroscopy was performed on I91–I98 in the presence and absence of αB-crystallin. A custom-built AFM setup was used that incorporated a commercial AFM head stage (Veeco Instruments, Mannheim, Germany) as described (19). The force transducer was a standard Si_3N_4 triangular cantilever (Veeco Instruments) whose stiffness was calibrated in solution for each separate experiment using the equipartition theorem and was nominally 40 piconewtons (pN)/nm to within 20%. In a typical experiment, 50 μl of 0.17 μg/ml I91–I98 in 0.1 M NaCl and 50 mM sodium phosphate (pH 7.0) was deposited onto a freshly coated gold coverslip (produced by evaporation of a 40-nm layer of nickel/chromium, followed by a 10-nm surface layer of gold) and allowed to adsorb onto the surface for 5 min before washing away unbound protein with excess buffer. Triangular input waveforms were applied to a z-piezo actuator (Physik Instrumente, Karlsruhe, Germany), resulting in five different stretch rates: 200, 400, 1000, 1500, and 3000 nm s^{-1}. Sawtooth data were acquired, and the peak forces were recorded (30). αB-crystallin was then added to the same sample at a molar ratio of ~130:1 (αB-crystallin/I91–I98) and not washed away. Because some fraction of the αB-crystallin molecules will bind to the gold, we estimated that the effective molar ratio of non-surface-bound αB-crystallin to I91–I98 was ~70:1 (~9 αB-crystallin molecules/Ig domain), with an error of at least 20%. Sawtooth data were then acquired at the same rates of stretch, and the peak forces were similarly recorded. In control experiments, excess protein kinase A (catalytic subunit from bovine heart) was added to I91–I98 instead of αB-crystallin; the effective molar ratio of protein kinase A to I91–I98 was ~60:1.

RESULTS

Position of αB-crystallin in Cardiac Fibers—The position of αB-crystallin in cardiac fibers relative to a particular region of I-band titin was determined by labeling the fibers with the antibody against αB-crystallin and the antibody S54/56 against Ig domains in the N2A region of the N2BA isoform of titin (Fig. 1). The fibers were stretched in relaxing conditions by varying amounts up to ~2.7 μm; Fig. 2 shows the positions of antibody labels at 2.0 and 2.5 μm. Anti-αB-crystallin antibody labeled in a line parallel to the Z-disc; and in stretched fibers, the line

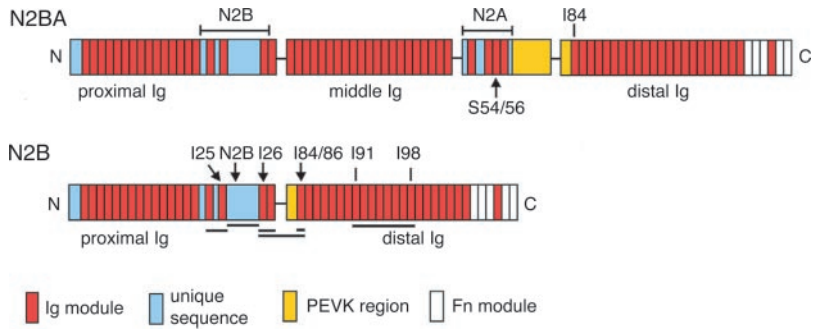

FIG. 1. **Sequence of cardiac I-band titin.** Cardiac muscle expresses a large N2BA isoform (*upper splicing pathway*) and a smaller N2B isoform (*lower splicing pathway*). The number of Ig domains in the middle Ig region of N2BA is variable. The positions of fragments used in binding studies are *underlined*: the N-terminal N2B region with Ig domains I24/I25, uN2B, Ig domains I26/I27, the PEVK domain flanked by Ig domains I26/I27 and I84, Ig domain I84, and Ig domains I91–I98. The epitopes of antibodies to I25, N2B, I26, I84/86, and S54/56 are marked by *arrows*. The diagram is modified from Ref. 13. *Fn*, fibronectin.

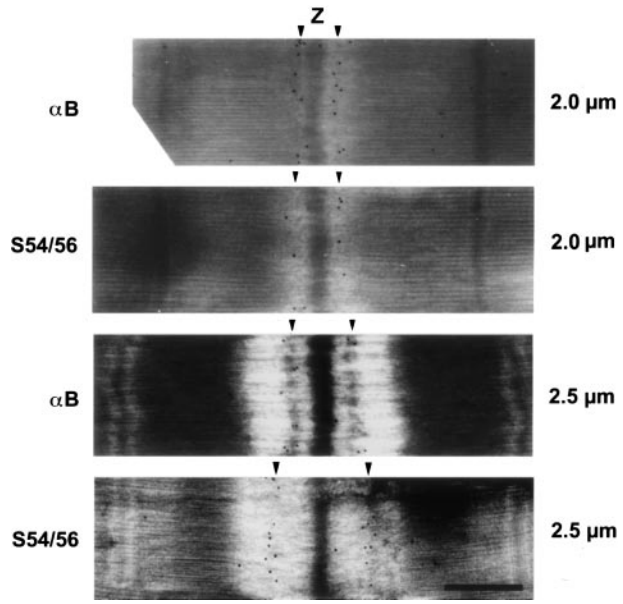

FIG. 2. **Electron micrographs showing the position of αB-crystallin relative to the N2A region of cardiac titin.** Cryosections of cardiac fibers at different sarcomere lengths were labeled with anti-αB-crystallin or S54/56 and protein A-gold. Sarcomere lengths of 2.0 and 2.5 μm are shown. In unstretched sarcomeres, αB-crystallin was slightly closer to the Z-disc (*Z*) than S54/56; in stretched sarcomeres, S54/56 was pulled farther from the Z-disc than αB-crystallin. *Scale bar* = 0.5 μm.

moved away from the Z-disc. This change in position of αB-crystallin as the sarcomere was extended is consistent with binding of αB-crystallin to titin. The S54/56 label was farther away from the Z-disc than αB-crystallin at 2.0-μm sarcomere length and moved even farther from the Z-disc than αB-crystallin in sarcomeres stretched to 2.5 μm. Because the N terminus of titin is in the Z-disc (12), these results show that αB-crystallin binds to a region of titin nearer the Z-disc than N2A. A more complete picture of the movement of αB-crystallin and the S54/56 epitope at different sarcomere lengths shows there is an extensible region between the epitope in N2A and αB-crystallin (Fig. 3).

Another approach to finding binding sites for αB-crystallin on titin was to add αB-crystallin back to cardiac myofibrils that had been skinned and to determine the position of the bound αB-crystallin from immunofluorescent images. Single myofibrils were stretched up to 3.5-μm sarcomere length and incubated first with αB-crystallin and then with anti-αB-crystallin. The skinning procedure removed endogenous αB-crystallin, and the antibody did not label untreated myofibrils. The separation of labeled sites on either side of the Z-disc was resolved at ~2.6-μm sarcomere length and increased as the sarcomere was stretched farther; the width of labeled stripes increased as the myofibril was stretched (Fig. 4*A*). In some myofibrils with overstretched sarcomeres, the chaperone bound in the region between the middle of the I-band and the Z-disc. Such a myofibril labeled with both anti-I25 and αB-crystallin is shown in Fig. 4*B*. In the overlay image, the I25 epitope (in the N-terminal part of the N2B region) is at the periphery of the broad αB-crystallin label. In these myofibrils, αB-crystallin is in the proximal Ig region. The PEVK domain would be considerably extended at long sarcomere lengths; and if αB-crystallin were bound to PEVK, a broad band of labeling C-terminal to I25 would be expected. This was not observed.

Values for the distance from the center of the Z-disc to the fluorescent antibody label obtained from myofibrils labeled with αB-crystallin (similar to those in Fig. 4*A*) were plotted on the same graph as the values obtained from electron micrographs of fibers labeled directly with anti-αB-crystallin (Fig. 3). A nearly continuous curve was obtained with measurements from electron micrographs at shorter sarcomere lengths, within the physiological range, and from fluorescent images at long sarcomere lengths. Thus, electron micrographs and immunofluorescent images show that αB-crystallin bound predominately to a region of titin nearer to the Z-disc than N2A in the N2BA isoform; αB-crystallin is therefore nearer the Z-disc than the PEVK domain in both isoforms. Antibodies to the N-terminal part of uN2B and to I26 and I84/86 were previously used to label rabbit cardiac fibers at different sarcomere lengths (15); the positions of these epitopes relative to αB-crystallin are shown in Fig. 3. As sarcomeres were stretched, the position of αB-crystallin coincided with the uN2B label and was clearly on the Z-disc side of I26, which co-localized with S54/56, in agreement with previous results (15). I26 and I84/86 are on either side of PEVK in the N2B isoform (Fig. 1), and both these epitopes were farther from the Z-disc than αB-crystallin in stretched sarcomeres. The extension of PEVK is shown by increasing separation of I26 and I84/86 (Fig. 3) (15); at corresponding sarcomere lengths, αB-crystallin remained on the Z-disc side of I26. These labeling results show that αB-crystallin is associated with the N2B region of titin and is nearer the Z-disc than the PEVK domain.

αB-crystallin Binding to Titin and Recombinant Fragments—Binding of αB-crystallin to the native titin molecule was tested by an immunoaffinity method. Antibody to titin domain I26 was immobilized on beads, and a mixture of αB-crystallin and titin was applied to the beads. αB-crystallin bound to beads in the presence (but not absence) of titin, and more αB-crystallin was bound at 42 °C than at 0 °C (Fig. 5),

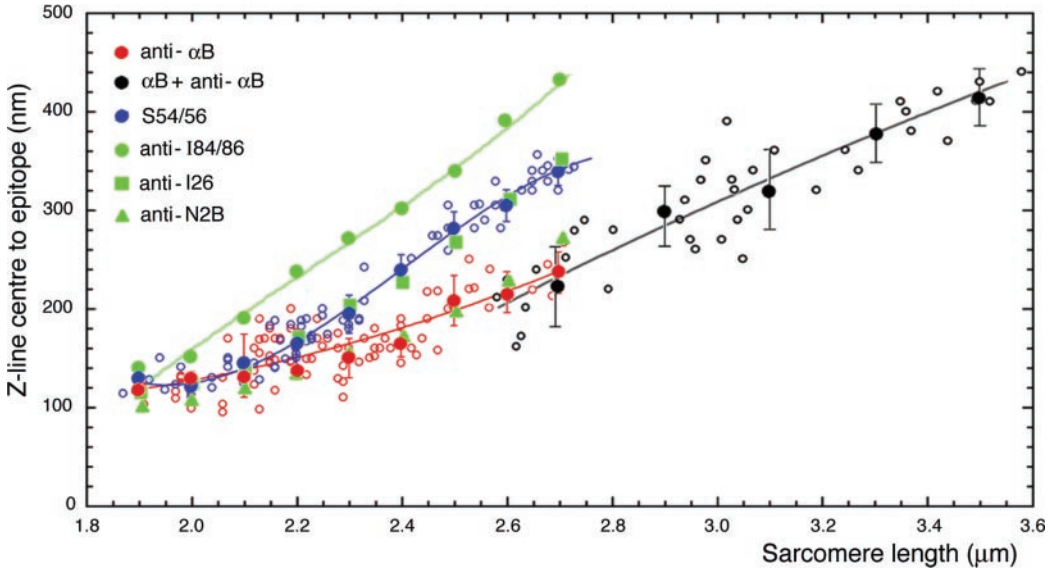

FIG. 3. **Positions of αB-crystallin and the N2A and N2B regions of cardiac titin at increasing sarcomere lengths.** Measurements were made from electron micrographs of cryosections of cardiac fibers labeled with anti-αB-crystallin or S54/56 (similar to those in Fig. 2). For these experiments, fibers were not stretched above sarcomere lengths of ~2.7 μm (*red* and *blue curves*). In a separate series of experiments, single myofibrils were incubated with αB-crystallin (*αB*), followed by anti-αB-crystallin (*anti-αB*) and fluorescent secondary antibody (as illustrated in Fig. 4). Myofibrils were stretched over a range of sarcomere lengths from 2.6 to ~3.5 μm (*black curve*). Data points for the positions of individual gold particles (*open circles*) and mean values (*closed circles*) are shown with S.D., calculated in bins of sarcomere lengths of 100 μm wide for immunoelectron micrographs and 200 μm wide for immunofluorescence. Data points were fitted by least-squares polynomial regression. Also shown are mean values for the positions of antibodies taken from immunoelectron microscopy and immunofluorescence measurements in Ref. 15 (*green symbols*).

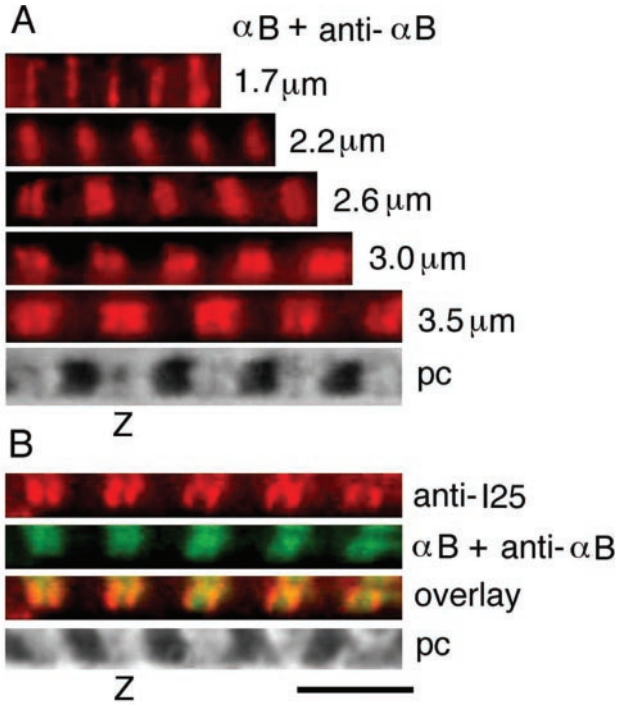

FIG. 4. **Fluorescence micrographs of stretched cardiac myofibrils showing the site of αB-crystallin binding.** *A*, single myofibrils were stretched to sarcomere lengths of up to 3.5 μm and incubated with αB-crystallin (*αB*), followed by anti-αB-crystallin (*anti-αB*). *B*, a myofibril was stretched to a sarcomere length of ~3.5 μm and double-labeled with anti-I25 and αB-crystallin, followed by anti-αB-crystallin. The phase-contrast images (*pc*) show that labeling is within the I-band in *A* and *B*. The secondary antibodies used were Cy3-conjugated anti-rabbit IgG in *A* and Cy3-conjugated anti-mouse IgG and fluorescein isothiocyanate-conjugated anti-rabbit IgG in *B*. *Z*, Z-disc. *Scale bar* = 5 μm.

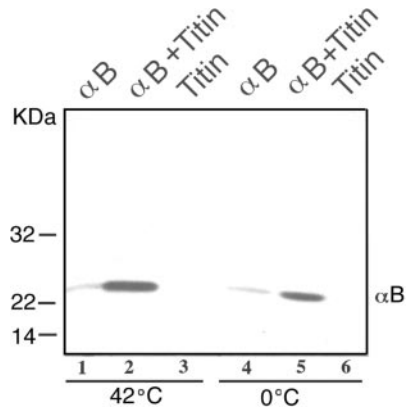

FIG. 5. **αB-crystallin binding to whole titin.** Shown is an immunoblot of samples eluted from protein A-Sepharose CL-4B beads coupled with antibody to Ig domain I26. αB-crystallin (*αB*) (*lanes 1* and *4*), a mixture of αB-crystallin and titin (*lanes 2* and *5*), or titin alone (*lanes 3* and *6*) was incubated at 4 or 0 °C and added to separate aliquots of the beads. A blot of protein eluted from the beads was incubated with anti-αB-crystallin. αB-crystallin in mixtures of αB-crystallin and titin was bound to the beads.

suggesting that the binding was at least partly hydrophobic.

Binding of αB-crystallin to recombinant fragments from different regions of titin was tested on immunoblots. An SDS-polyacrylamide gel of the fragments is shown in Fig. 6*A*, with a corresponding blot of the same proteins incubated with αB-crystallin, followed by anti-αB-crystallin (Fig. 6*B*). αB-crystallin bound strongly to uN2B and to the two Ig domains C-terminal to uN2B (I26/I27) and less strongly to the PEVK fragment (I26/I27–I84), but did not bind to the two Ig domains near the N terminus of N2B (I24/I25) or to the Ig domain C-terminal to the PEVK domain (I84). A block of eight Ig domains (I91–I98) from the distal tandem Ig region has been used as a model titin fragment for studying the stability of Ig domains (19, 24, 31). αB-crystallin bound only weakly to these Ig domains on the immunoblot. αB-crystallin binding to a fragment of the PEVK domain in skeletal muscle titin was also tested; the protein was partially degraded because it lacks stabilizing Ig domains at each end. αB-crystallin did not bind to this PEVK fragment. Because the proteins were denatured by

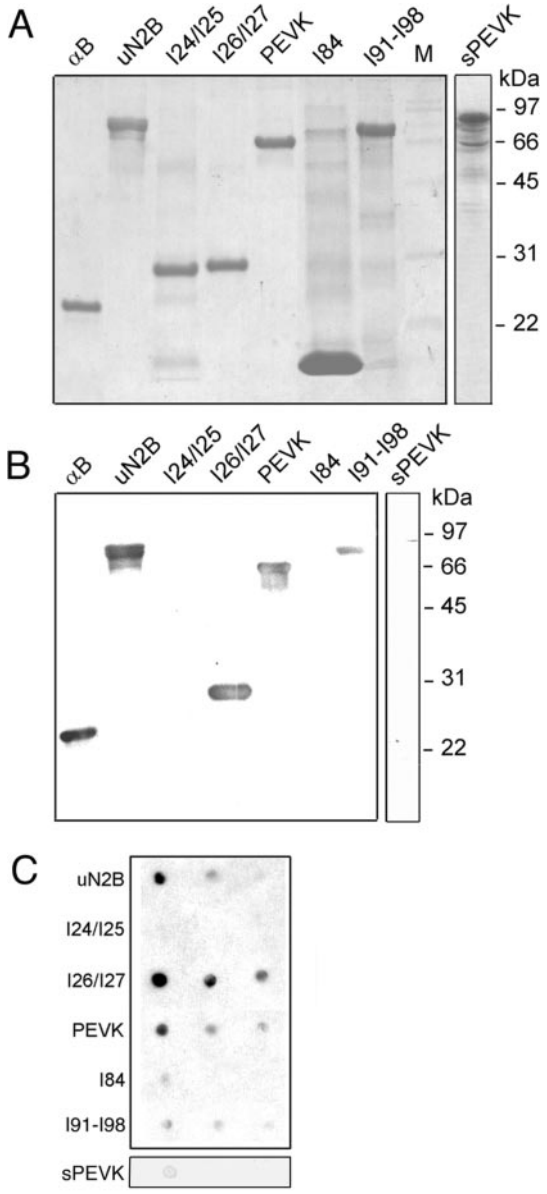

FIG. 6. **Binding of αB-crystallin to different regions of I-band titin.** *A*, SDS-polyacrylamide gel of recombinant fragments used in the binding assay. Equal amounts of fragments were loaded onto the gel, except for I84, for which five times as much was loaded to compensate for losses of this low molecular mass protein during immunoblotting. *B*, immunoblot of a gel similar to the one in *A*. *C*, dot blot of the same fragments. Spots of each fragment have 10, 5, and 2.5 ng of protein. Blots were incubated with αB-crystallin (*αB*), followed by anti-αB-crystallin and secondary antibody. *sPEVK*, skeletal PEVK.

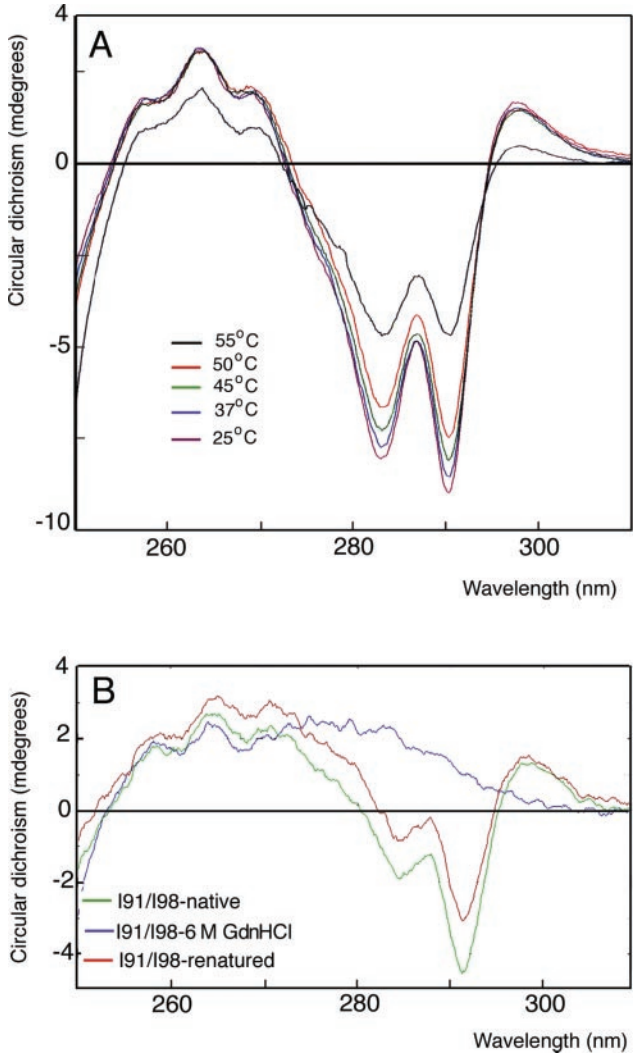

FIG. 7. **Stability of I91–I98 under denaturing conditions.** *A*, effect of temperature on the near-UV CD spectrum. Spectra of I91–I98 (1.5 mg/ml) were measured at the temperatures shown. *B*, reversible denaturation of I91–I98 (1.0 mg/ml) by GdnHCl. Spectra of I91–I98 were measured for the native protein, in the presence of 6 M GdnHCl, and after returning to native conditions. The path length of the cell was 10 mm in *A* and *B*. The CD signal is lower in *B* than *A* because the concentration of protein was lower.

SDS before running on the gel, it is possible that the binding was not representative of binding to the native protein. Therefore, the reaction of αB-crystallin with the titin fragments was also tested on a dot blot of the native proteins (Fig. 6*C*). The result was the same as described for the blot of the SDS-polyacrylamide gel, but αB-crystallin bound to I26/I27 more strongly that to the other fragments. Binding of αB-crystallin to the fragments giving a positive result on blots was tested by several pull-down assays in which either αB-crystallin or the fragments were bound to beads. None of the pull-down assays showed convincing binding of αB-crystallin to any of these titin fragments, probably because binding was too weak to be detected reliably by this method. The recombinant cardiac PEVK fragment has Ig domains I26/I27 at the N terminus and Ig domain I84 at the C terminus to provide stability (Fig. 1). The binding of αB-crystallin to this protein is likely to be through I26/I27 because αB-crystallin binds to these domains and not to I84. The lack of binding between αB-crystallin and the skeletal PEVK fragment supports this interpretation and makes it unlikely that the chaperone binds to the cardiac PEVK sequence. The antibody labeling pattern in fibers shows that the chaperone did not bind to cardiac PEVK *in situ*.

Stability of I91–I98—The lack of αB-crystallin binding to the distal Ig region in highly stretched muscle fibers suggests that Ig domains in this part of titin are particularly stable. The stability of I91–I98 was investigated by following the change from the native structure by measuring the near-UV CD spectrum at different temperatures (Fig. 7*A*). The CD spectrum had distinct minima at 283 and 290 nm, which decreased slightly as the temperature was raised from 25 to 50 °C, showing there was a small change in the tertiary structure of Ig domains. The sharp drop in the CD spectrum at 55 °C suggests there was a more significant change at this temperature and perhaps some aggregation. It was not possible to measure the effect of αB-

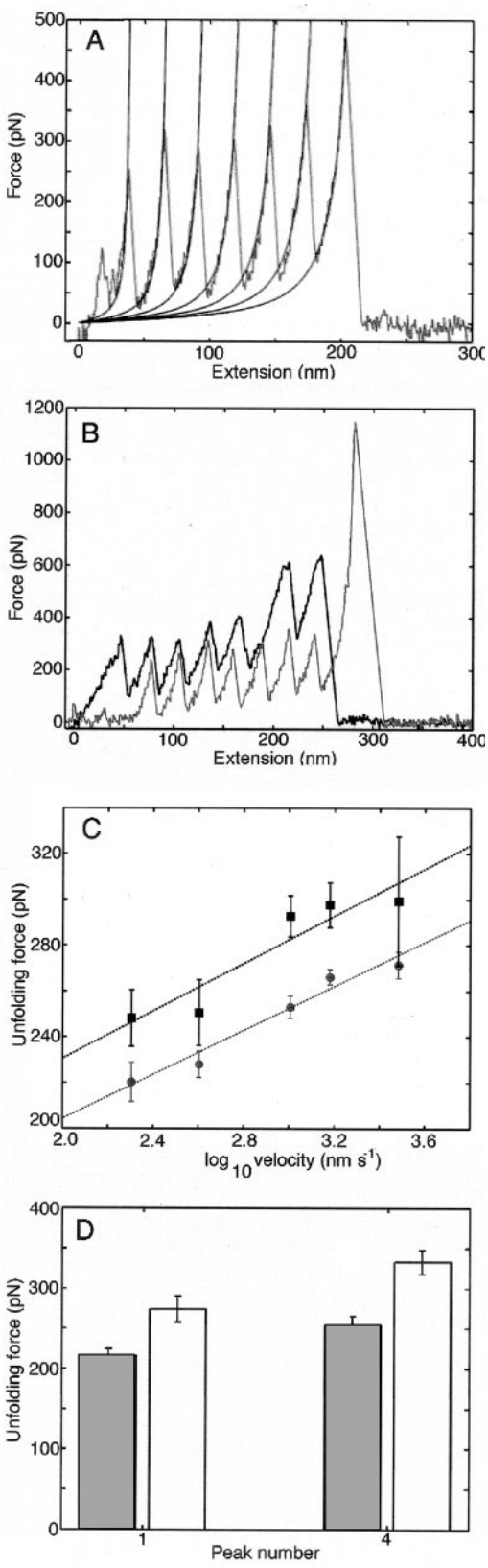

FIG. 8. **Effect of αB-crystallin on the stability of I91–I98.** *A*, force extension trace of I91–I98 in buffer alone (*gray curve*) taken at a stretch rate of 1500 nm s^{-1}. Predictions based on worm-like chain fits to the force extension trace preceding each force peak are shown (*black curve*), suggesting a spacing in contour length of 29 nm. *B*, typical force extension traces taken in the absence (*gray curve*) and presence (*black curve*) of αB-crystallin at a stretch rate of 1000 nm s^{-1}. *C*, variation of the pooled unfolding forces as a function of log of stretch rate in the absence (*circles*) and presence (*squares*) of αB-crystallin, with linear regression fits (*dashed lines*). *Errors bars* are S.E. *D*, histogram of mean unfolding forces for the first and fourth force peaks in the absence (*gray bars*) and presence (*white bars*) of αB-crystallin, collated at a stretch rate of 1000 nm s^{-1}. *Error bars* are one S.E. *Numbers* in each data set are 131, 81, 45, and 21 from left to right.

crystallin on denaturation at 55 °C because the chaperone itself is denatured at this temperature. I91–I98 lost tertiary structure in 6 M GdnHCl, as shown by the complete absence of the two near-UV CD minima in this denaturing agent (Fig. 7*B*). However, the CD spectrum returned fairly closely to the original value when the protein was renatured by removing GdnHCl. Thus, the eight Ig domains in I91–I98 are extremely stable to heat denaturation and spontaneously refold when GdnHCl is removed, without the need for αB-crystallin.

Effect of αB-crystallin on the Stability of Ig Domains—A stabilizing effect of αB-crystallin on Ig domains in I91–I98 was demonstrated by single molecule force spectroscopy. When I91–I98 molecules are stretched, consecutive Ig domains unfold, giving a sawtooth pattern of peak forces (24). I91–I98 molecules were stretched at five different rates, and the peak forces of the sawtooth pattern were recorded. Fig. 8*A* shows a representative force extension trace for I91–I98 stretched at 1500 nm s^{-1} in the absence of αB-crystallin, with fits overlaid according to worm-like chain predictions (24). Six sawtooth peaks are seen with forces in the range of 250–350 pN, corresponding to the unfolding of six of the eight Ig domains; the final peak at ~500 pN is due to detachment of the protein tether between the cantilever and cover glass. The worm-like chain model predicted that, upon unfolding of each Ig domain, the contour length of I91–I98 would increase by 27–30 nm; this value is comparable with that found for stretches of Ig modular peptides using both AFM (19, 24, 31) and laser tweezers (32, 33). Fig. 8*B* shows overlaid force extension traces obtained in the presence and absence of αB-crystallin employing the same stretch rate of 1000 nm s^{-1}. The unfolding force level of individual Ig domains is typically higher in the presence of αB-crystallin than in buffer alone. No significant change in the increase in contour length between force peaks was observed. Experiments in which protein kinase A was added in excess to I91–I98 produced no change in the unfolding force of Ig domains (data not shown). Pooling all peak force data for each stretch rate suggested that mean unfolding forces were 30–40 pN higher in the presence of αB-crystallin at equivalent stretch rates, although there was a relatively broad distribution of unfolding forces (Fig. 8*C*). This broad distribution is similar to that observed previously for I91–I98 (19, 31) and is indicative of heterogeneity in the mechanical properties of the eight individual Ig domains. To minimize this effect, we compared the unfolding forces in just the first and fourth peaks in each sawtooth pattern because individual Ig domains will, on average, have hierarchical unfolding forces dependent upon their relative mechanical stabilities.

Collating data from just one stretch rate of 1000 nm s^{-1} showed there was a significant difference ($p < 0.05$, Student's *t* test) between the unfolding forces of both the first and fourth peaks in the force extension traces of I91–I98 obtained in the presence and absence of αB-crystallin (Fig. 8*D*); these differences were 38 ± 2 and 59 ± 3 pN (mean ± S.E.), respectively. Calculations (34) from the linear fits to the pooled data of Fig. 8*C* show that the spontaneous rate of unfolding, averaged over all eight Ig domains in the titin construct, was lower in the presence of αB-crystallin than in buffer alone by a factor of ~3. Therefore, the presence of αB-crystallin substantially reduces the probability of Ig domain unfolding.

DISCUSSION

αB-crystallin binds to cardiac myofibrils under conditions that produce ischemia (7). Titin is a target for the chaperone, and the isolated protein will bind αB-crystallin even when not denatured. Antibody labeling in sectioned fibers showed that, within the physiological range of sarcomere lengths (1.9–2.4 μm), αB-crystallin was associated with a discrete region of titin, which moved away from the Z-disc as titin was extended. Contrary to expectation, αB-crystallin was not associated with the PEVK domain, but was in the N2B region. At longer sarcomere lengths, αB-crystallin added back to skinned myofibrils had a more diffuse distribution centered on the N2B region, which was probably due to extension of this sequence. Ig domains in the proximal Ig region of cardiac titin are known to be less stable than those in the distal region (19, 31). Some proximal Ig domains are predicted to unfold at the high end of the physiological range of sarcomere lengths, whereas Ig domains in the distal Ig region would unfold only at sarcomere lengths above ~6 μm (19). The spread of αB-crystallin up to the Z-disc in some overstretched myofibrils (Fig. 4*B*) is likely to be due to association of the chaperone with partially unfolded Ig domains in the proximal region.

The stability of the block of eight Ig domains (I91–I98) from the distal Ig region was shown by resistance to denaturation upon heating and spontaneous refolding to the nearly native state after renaturation from GdnHCl. αB-crystallin would not be expected to associate with these relatively stable Ig domains under physiological conditions. An unexpected finding was that αB-crystallin bound to Ig domains I26/I27 at the C-terminal end of the N2B region under mild conditions when it did not bind to other Ig domains. This suggests that one or both of these Ig domains is relatively unstable, although we cannot exclude the possibility that αB-crystallin binds to folded I26/I27. I27 is in all isoforms of titin (except the minor isoform Novex-3, which is not a full-length titin), and an individual exon codes for this domain (14). If I27 were responsible for αB-crystallin binding to I26/I27 and the domain were unusually unstable, it might have an important function in titin elasticity, possibly modulating the extension of the uN2B sequence upon stretch. (I27 in the new nomenclature is not to be confused with I27 in the old nomenclature, which is now called I91. I91 is stable.)

The binding of αB-crystallin to the N2B region of cardiac titin in only moderately stretched fibers suggests that this part of titin is particularly vulnerable to misfolding at physiological sarcomere lengths. The N2B region in cardiac muscle binds metabolic enzymes via a LIM protein, DRAL/FHL-2 (35); this important function may need a specific conformation of the central region of the uN2B sequence, which may be protected by αB-crystallin under conditions of stress. The binding of αB-crystallin to recombinant titin fragments from the N2B region shows that the chaperone binds directly to titin and therefore probably not via the enzymes or DRAL/FHL-2.

AFM measurements showed that αB-crystallin stabilizes Ig domains. When single molecules of I91–I98 were stretched, Ig domains unfolded consecutively, and the force needed to unfold individual domains was greater in the presence of αB-crystallin. Because the Ig domains in I91–I98 vary in stability, the significance of this effect was demonstrated individually for the first and fourth sawtooth force peaks. αB-crystallin was found to decrease the probability of Ig domain unfolding. Under conditions of stress, when spontaneous unfolding of Ig domains would be more likely, recruitment of αB-crystallin to Ig regions of titin would have a stabilizing effect. This would be especially important in the more labile proximal Ig region.

αB-crystallin, like other sHSPs, binds to proteins that have lost all or part of their secondary structure and prevents the irreversible formation of aggregates, but it does not have the usual chaperone activity of assisting refolding, which requires ATP (4, 36, 37). The 20-kDa monomers of αB-crystallin form complexes with molecular masses of 300–800 kDa; the structure of the complex is variable, and exchange of subunits between complexes suggests that the oligomer is unstable (38, 39). Recombinant αB-crystallin has a chaperone function similar to that of the native protein (25), but it forms complexes that are more uniform in size than the native protein. Reconstruction of cryoelectron microscope images of selected particles showed that the roughly spherical complex is ~10 nm in diameter, with protein subunits surrounding a central cavity (40). The variability in size and shape of the protein shell suggests that the αB-crystallin monomer is flexible. αB-crystallin and other sHSPs have an "α-crystallin domain" in the C-terminal region that consists of β-strands in an Ig fold (41, 42). The Ig domain has been confirmed in the crystal structures of two sHSPs (43, 44). Target proteins are bound to αB-crystallin at the α-crystallin domain and also at the hydrophobic N-terminal region, which is inside the complex (36). The dynamic nature of the oligomers of sHSPs has led to the proposal that, under unfavorable conditions, there is transient dissociation of oligomers, which allows partially unfolded target proteins to bind to sites usually unavailable within the complex (42, 43).

A model derived from studies of the binding of αA- and αB-crystallins to mutant lysozymes of varying stability (45, 46) can be applied to the association of αB-crystallin with titin. α-Crystallins recognize proteins in states intermediate between the native and completely unfolded states. Two modes of binding between α-crystallins and substrates have been identified: a low capacity, high affinity mode binding to the more nearly native substrates and a high capacity, low affinity mode binding to more destabilized substrates. The low affinity binding to less native substrates prevents the chaperones from promoting protein unfolding. The extremely low affinity of αB-crystallin for completely unfolded states would explain the lack of binding to the PEVK domain of titin that we observed in immunoelectron microscope and immunofluorescent images and in binding assays with PEVK from skeletal titin. Binding of αB-crystallin to the uN2B sequence suggests that this region has appreciable secondary structure *in vivo*. As discussed above, differential binding of αB-crystallin to Ig domains would reflect the relative stabilities of these domains. αB-crystallin could bind reversibly to proximal tandem Ig domains if a few were partially unfolded at physiological sarcomere lengths, and this would protect them from further unfolding.

Association of substrates with α-crystallins is dynamic, and the equilibrium between binding to the chaperone and dissociation and refolding depends on prevailing conditions and the oligomeric state of the α-crystallin. The capacity and affinity of αB-crystallin for partially unfolded substrates are increased by phosphorylation in the N-terminal region, which destabilizes the structure of the oligomer, promoting substrate binding; this is thought to regulate αB-crystallin chaperone activity (45, 47). About 20% of the total αB-crystallin is phosphorylated when the protein moves to myofibrils under conditions of stress (7). In cardiac fibers, β-adrenergic stimulation produces an increase in the frequency of contractions, which is due to phosphorylation of myofibrillar proteins such as troponin I and myosin-binding protein C by cAMP-dependent protein kinase (48–50). Rat heart titin is phosphorylated in the uN2B sequence following β-adrenergic stimulation, and this produces a drop in passive tension (51). αB-crystallin is phosphorylated by cAMP-dependent protein kinase (52), and activation of the

enzyme would be expected to increase the affinity of αB-crystallin for the N2B sequence as well as phosphorylating N2B itself. Thus, αB-crystallin may protect this region from potential damage incurred when a more compliant uN2B sequence is stretched.

In conclusion, αB-crystallin binds to cardiac titin in the N2B region at physiological sarcomere lengths. Binding sites are in the uN2B sequence and I26/I27. At longer sarcomere lengths, αB-crystallin can also bind to the proximal Ig region. Previous work has shown that αB-crystallin moves to sites on myofibrils under conditions of stress, including ischemia. The function of αB-crystallin is likely to be the protection of the extensible N2B region and less stable Ig domains from denaturation due to unfolding, by binding reversibly to intermediate folding states.

REFERENCES

1. Horwitz, J. (1992) *Proc. Natl. Acad. Sci. U. S. A.* **89,** 10449–10453
2. Jaenicke, R., and Slingsby, C. (2001) *Crit. Rev. Biochem. Mol. Biol.* **36,** 435–499
3. Bhat, S. P., and Nagineni, C. N. (1989) *Biochem. Biophys. Res. Commun.* **158,** 319–325
4. Horwitz, J. (2000) *Semin. Cell Dev. Biol.* **11,** 53–60
5. Ray, P. S., Martin, J. L., Swanson, E. A., Otani, H., Dillmann, W. H., and Das, D. K. (2001) *FASEB J.* **15,** 393–402
6. Martin, J. L., Mestril, R., Hilal-Dandan, R., Brunton, L. L., and Dillmann, W. H. (1997) *Circulation* **96,** 4343–4348
7. Golenhofen, N., Htun, P., Ness, W., Koob, R., Schaper, W., and Drenckhahn, D. (1999) *J. Mol. Cell. Cardiol.* **31,** 569–580
8. van de Klundert, F. A., Gijsen, M. L., van den Ijssel, P. R., Snoeckx, L. H., and de Jong, W. W. (1998) *Eur. J. Cell Biol.* **75,** 38–45
9. Barbato, R., Menabo, R., Dainese, P., Carafoli, E., Schiaffino, S., and Di Lisa, F. (1996) *Circ. Res.* **78,** 821–828
10. Golenhofen, N., Arbeiter, A., Koob, R., and Drenckhahn, D. (2002) *J. Mol. Cell. Cardiol.* **34,** 309–319
11. Gregorio, C. C., Granzier, H., Sorimachi, H., and Labeit, S. (1999) *Curr. Opin. Cell Biol.* **11,** 18–25
12. Fürst, D. O., Osborn, M., Nave, R., and Weber, K. (1988) *J. Cell Biol.* **106,** 1563–1572
13. Freiburg, A., Trombitas, K., Hell, W., Cazorla, O., Fougerousse, F., Centner, T., Kolmerer, B., Witt, C., Beckmann, J. S., Gregorio, C. C., Granzier, H., and Labeit, S. (2000) *Circ. Res.* **86,** 1114–1121
14. Bang, M. L., Centner, T., Fornoff, F., Geach, A. J., Gotthardt, M., McNabb, M., Witt, C. C., Labeit, D., Gregorio, C. C., Granzier, H., and Labeit, S. (2001) *Circ. Res.* **89,** 1065–1072
15. Linke, W. A., Rudy, D. E., Centner, T., Gautel, M., Witt, C., Labeit, S., and Gregorio, C. C. (1999) *J. Cell Biol.* **146,** 631–644
16. Helmes, M., Trombitas, K., Centner, T., Kellermayer, M., Labeit, S., Linke, W. A., and Granzier, H. (1999) *Circ. Res.* **84,** 1339–1352
17. Neagoe, C., Kulke, M., del Monte, F., Gwathmey, J. K., de Tombe, P. P., Hajjar, R. J., and Linke, W. A. (2002) *Circulation* **106,** 1333–1341
18. Granzier, H., and Labeit, S. (2002) *J. Physiol. (Lond.)* **541,** 335–342
19. Li, H., Linke, W. A., Oberhauser, A. F., Carrion-Vazquez, M., Kerkvliet, J. G., Lu, H., Marszalek, P. E., and Fernandez, J. M. (2002) *Nature* **418,** 998–1002
20. Soteriou, A., Gamage, M., and Trinick, J. (1993) *J. Cell Sci.* **104,** 119–123
21. Linke, W. A., Kulke, M., Li, H., Fujita-Becker, S., Neagoe, C., Manstein, D. J., Gautel, M., and Fernandez, J. M. (2002) *J. Struct. Biol.* **137,** 194–205
22. Kulke, M., Fujita-Becker, S., Rostkova, E., Neagoe, C., Labeit, D., Manstein, D. J., Gautel, M., and Linke, W. A. (2001) *Circ. Res.* **89,** 874–881
23. Yamasaki, R., Berri, M., Wu, Y., Trombitas, K., McNabb, M., Kellermayer, M. S., Witt, C., Labeit, D., Labeit, S., Greaser, M., and Granzier, H. (2001) *Biophys. J.* **81,** 2297–2313
24. Rief, M., Gautel, M., Oesterhelt, F., Fernandez, J. M., and Gaub, H. E. (1997) *Science* **276,** 1109–1112
25. Horwitz, J., Huang, Q. L., Ding, L., and Bova, M. P. (1998) *Methods Enzymol.* **290,** 365–383
26. Gautel, M., Lehtonen, E., and Pietruschka, F. (1996) *J. Muscle Res. Cell Motil.* **17,** 449–461
27. Linke, W. A., Ivemeyer, M., Olivieri, N., Kolmerer, B., Rüegg, J. C., and Labeit, S. (1996) *J. Mol. Biol.* **261,** 62–71
28. Linke, W. A., Ivemeyer, M., Labeit, S., Hinssen, H., Rüegg, J. C., and Gautel, M. (1997) *Biophys. J.* **73,** 905–919
29. Lakey, A., Ferguson, C., Labeit, S., Reedy, M., Larkins, A., Butcher, G., Leonard, K., and Bullard, B. (1990) *EMBO J.* **9,** 3459–3467
30. Linke, W. A., and Fernandez, J. M. (2002) *J. Muscle Res. Cell Motil.* **23,** 483–497
31. Watanabe, K., Mühle-Goll, C., Kellermayer, M. S., Labeit, S., and Granzier, H. (2002) *J. Struct. Biol.* **137,** 248–258
32. Tskhovrebova, L., Trinick, J., Sleep, J. A., and Simmons, R. M. (1997) *Nature* **387,** 308–312
33. Leake, M. C., Wilson, D., Bullard, B., and Simmons, R. M. (2003) *FEBS Lett.* **535,** 55–60
34. Carrion-Vazquez, M., Oberhauser, A. F., Fowler, S. B., Marszalek, P. E., Broedel, S. E., Clarke, J., and Fernandez, J. M. (1999) *Proc. Natl. Acad. Sci. U. S. A.* **96,** 3694–3699
35. Lange, S., Auerbach, D., McLoughlin, P., Perriard, E., Schafer, B. W., Perriard, J. C., and Ehler, E. (2002) *J. Cell Sci.* **115,** 4925–4936
36. Derham, B. K., and Harding, J. J. (1999) *Prog. Retinal Eye Res.* **18,** 463–509
37. Horwitz, J. (2003) *Exp. Eye Res.* **76,** 145–153
38. van den Oetelaar, P. J., van Someren, P. F., Thomson, J. A., Siezen, R. J., and Hoenders, H. J. (1990) *Biochemistry* **29,** 3488–3493
39. Bova, M. P., Ding, L. L., Horwitz, J., and Fung, B. K. (1997) *J. Biol. Chem.* **272,** 29511–29517
40. Haley, D. A., Horwitz, J., and Stewart, P. L. (1998) *J. Mol. Biol.* **277,** 27–35
41. Mornon, J. P., Halaby, D., Malfois, M., Durand, P., Callebaut, I., and Tardieu, A. (1998) *Int. J. Biol. Macromol.* **22,** 219–227
42. Koteiche, H. A., and McHaourab, H. S. (1999) *J. Mol. Biol.* **294,** 561–577
43. Kim, R., Kim, K. K., Yokota, H., and Kim, S. H. (1998) *Proc. Natl. Acad. Sci. U. S. A.* **95,** 9129–9133
44. van Montfort, R. L., Basha, E., Friedrich, K. L., Slingsby, C., and Vierling, E. (2001) *Nat. Struct. Biol.* **8,** 1025–1030
45. Koteiche, H. A., and McHaourab, H. S. (2003) *J. Biol. Chem.* **278,** 10361–10367
46. McHaourab, H. S., Dodson, E. K., and Koteiche, H. A. (2002) *J. Biol. Chem.* **277,** 40557–40566
47. Ito, H., Kamei, K., Iwamoto, I., Inaguma, Y., Nohara, D., and Kato, K. (2001) *J. Biol. Chem.* **276,** 5346–5352
48. Gruen, M., Prinz, H., and Gautel, M. (1999) *FEBS Lett.* **453,** 254–259
49. Kentish, J. C., McCloskey, D. T., Layland, J., Palmer, S., Leiden, J. M., Martin, A. F., and Solaro, R. J. (2001) *Circ. Res.* **88,** 1059–1065
50. Kunst, G., Kress, K. R., Gruen, M., Uttenweiler, D., Gautel, M., and Fink, R. H. (2000) *Circ. Res.* **86,** 51–58
51. Yamasaki, R., Wu, Y., McNabb, M., Greaser, M., Labeit, S., and Granzier, H. (2002) *Circ. Res.* **90,** 1181–1188
52. Kantorow, M., and Piatigorsky, J. (1994) *Proc. Natl. Acad. Sci. U. S. A.* **91,** 3112–3116